Determination of radionuclide speciation in aqueous solutions by EXAFS spectroscopy

T. Reich, L. Baraniak, G. Bernhard, H. Funke, G. Geipel, C. Hennig, A. Roßberg
Forschungszentrum Rossendorf e.V., Institute of Radiochemistry, Dresden, Germany

Introduction

A significant part of environmental research on radionuclides is devoted to the determination of fundamental parameters that allow to understand and to predict the migration behavior of radionuclides in the bio- and geosphere. Almost every radionuclide interaction in the environment involves aqueous systems, e.g., complex formation with dissolved organic substances, colloid formation, sorption onto mineral surfaces, interaction with microorganisms, dissolution and precipitation, and redox reactions [1].

Extended X-ray absorption fine structure (EXAFS) spectroscopy is a powerful tool for the determination of molecular-level information on the speciation of radionuclides in aqueous solutions. The speciation not only describes the type of the radionuclide and its concentration but also its oxidation state and coordination sphere. The structural parameters of the radionuclide surrounding, i.e., bond distances, coordination numbers, and type of neighboring atoms, can be determined by EXAFS spectroscopy. The X-ray absorption near-edge structure (XANES) contains information on the electronic structure and the molecular symmetry of the radionuclide.

Although EXAFS and XANES spectroscopies have demonstrated their potentials in many areas of research since the mid seventies, they were rarely used in radionuclide studies until the mid nineties. Only then it became possible at a few synchrotron light sources in the world to implement protocols and procedures allowing to handle radionuclides safely at large multi-user facilities. However, these protocols impose restrictions on the activity and type of radionuclides that can be studied and do not, usually, allow for any sample manipulation.

The Rossendorf Beamline (ROBL) is unique in that sense that it operates the first experimental station dedicated to X-ray absorption spectroscopy on radionuclides at a synchrotron light source in Europe. At ROBL it is possible to study solid and liquid radionuclide samples of the following actinides Th-nat, Pa-231, U-nat, Np-237, Pu-239, Pu-242, Am-241, Am-243 as well as Ra-226, Po-208, and Tc-99 [2]. The maximal total activity authorized to be at ROBL at any given time is 185 MBq (5 mCi). In addition to all the advantages offered by a third-generation synchrotron light source as the ESRF, the uniqueness of ROBL is also due to the possibility of sample manipulation in a specially designed glove box before or during the measurement.

The first X-ray absorption spectra of uranium sample were collected at ROBL in August 1998 followed by the first X-ray absorption fine structure (XAFS) measurements on neptunium and technetium samples in November 1998. Since the beamline was still in commissioning at that time, some of the experiments were designed to test ROBL's technical capabilities for XAFS measurements. Due to the importance of radionuclide speciation in aqueous systems mentioned above, this report will highlight some results obtained on solutions of Np, Tc, and U using XAFS spectroscopy and illustrate the type of information that can be obtained at ROBL.

Experimental

This section describes briefly sample preparation, data collection and data analysis. More details are given in the corresponding Experimental Reports at the end of this report. For EXAFS measurements on liquid samples, 4 ml of the solution was filled in a polyethylene cuvette, which was sealed and put in a polyethylene bag. Multiple scans of the EXAFS were

collected at room temperature using the Si(111) double-crystal monchromator [2, this report, p.5]. The energy scale was calibrated using the first inflection point of the absorption spectra of various metal foils. The data were analyzed according to standard procedures [3] using the software EXAFSPAK [4]. Theoretical scattering phases and amplitudes were calculated using the scattering code FEFF6 [5].

Neptunium samples

A series of aqueous solutions containing 50 mM Np in three different oxidation states was prepared by dissolving solid $NpO_2(NO_3)$ in 0.1 M HNO_3. The isotope used was Np-237. Solution Np1 consisted of 50 mM Np(IV) in 0.1 M HNO_3 and 2 M H_2SO_4. The sulfuric acid was added to stabilize the Np(IV) oxidation state in the solution. The composition of solutions Np2 and Np3 was 50 mM Np(V) and Np(VI), respectively, in 0.1 M HNO_3. The different oxidation states of Np were obtained by electrochemical oxidation/reduction in a conventional H-formed electrolysis cell with a diaphragm between anode and cathode.

Technetium samples

Technetium Tc-99m is an important imaging agent in tumor diagnostic. EXAFS structural analysis of novel Tc complexes, which are synthesized by the Institute of Bioinorganic and Radiopharmaceutical Chemistry of the FZR, is the topic of intensive collaboration with the Institute of Radiochemistry [6, 7]. For Tc complexes, which do not form single crystals or do only exist in solutions, EXAFS spectroscopy is the only method that allows to obtain structural parameters of the near-neighbor surrounding of Tc. In order to evaluate the possibilities of ROBL's radiochemistry station for future EXAFS studies on Tc samples, two solutions were prepared for a first experiment with Tc-99 at ROBL. The amount of Tc in the concentrated sample with 127 mM $NaTcO_4$(aq) yielded an edge jump of ~1 across the Tc K-edge at 21 keV. The second sample was 100 times more dilute, i.e., the Tc concentration was 1.3 mM. This sample was measured in fluorescence mode using a quad pixel Ge fluorescence detector [8].

Uranium samples

Protocatechuic acid (PCA, 3,4-dihydroxy-benzoic acid) forms strong complexes with U(VI) and is an important wood degradation product present in waters of flooded uranium mines. The species distribution for 1 mM U(VI) and 50 mM PCA at I = 0.1 M was calculated under exclusion of CO_2 using the complexation constants determined by potentiometric pH titration [9] (see Fig. 1). The pH titration curves were evaluated assuming several 1:1, 1:2 and 1:3 uranyl complexes with PCA as indicated in Fig. 1. To validate these assumptions and to determine the role of the carboxylic COOH group and of the two phenolic OH groups of PCA in the complexation, seven solutions containing 1 mM $UO_2(ClO_4)_2$ and 50 mM PCA at different pH ranging from 4.30 to 6.75 were prepared under inert atmosphere for EXAFS measurements.

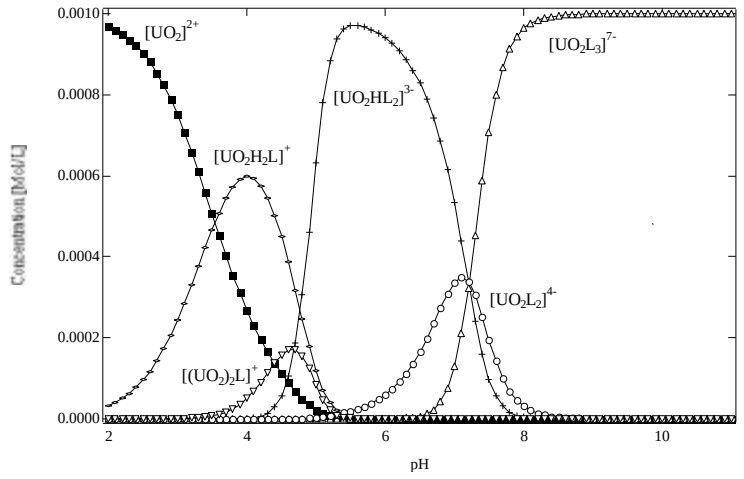

Fig. 1: Calculated species distribution of uranium as a function of pH in 50 mM PCA and I = 0.1 M.

Results and Discussion

Np(IV), Np(V), and Np(VI) solutions

Figure 2 shows the normalized Np L(III)-edge XANES spectra of 50 mM Np solutions of the different Np oxidation states IV, V, and VI. In contrast to Np(IV), Np in its oxidation states V and VI is known to form trans dioxo cations. This is the reason why the Np L(III)-edge XANES spectra of Np(V) and Np(VI) have a similar shape, which significantly differs from that of Np(IV). As can be seen from Fig. 2, the increase in the formal oxidation state from V to VI leads to a small shift of the absorption edge by 2.5 eV toward higher energy. The observed spectral features allow to distinguish between these three different Np oxidation states by Np L(III)-edge XANES spectroscopy.

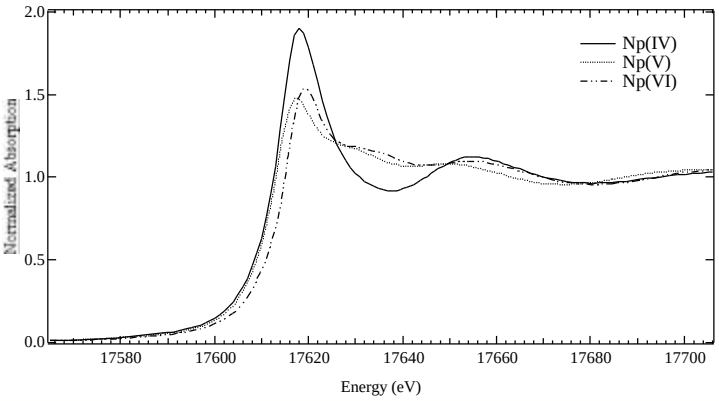

Fig. 2: Normalized Np L(III)-edge XANES spectra of 50 mM Np solutions.

In addition to the XANES spectra, information on the molecular structure is also contained in the EXAFS where it can be extracted in a quantitative way as several structural parameters. The raw EXAFS data and the best theoretical fit for solutions Np1-Np3 are shown in Fig. 3. The obtained structural parameters are given in Tab. 1. In solution Np1 Np(IV) is surrounded by 11 oxygen atoms at a distance of 2.39 Å. In the second coordination sphere we observed two sulfur atoms with a Np-S distance of 3.07 Å. This distance corresponds to a bidentate coordination of the SO_4^{2-} ion to the Np. Using the measured Np-O distance of 2.39 Å and the structural parameters of the SO_4^{2-} unit (S-O = 1.51 Å, angle O-S-O = 109^o [10]), the calculated Np-S distance of 2.93 Å is in good agreement with the measured value of 3.07 Å.

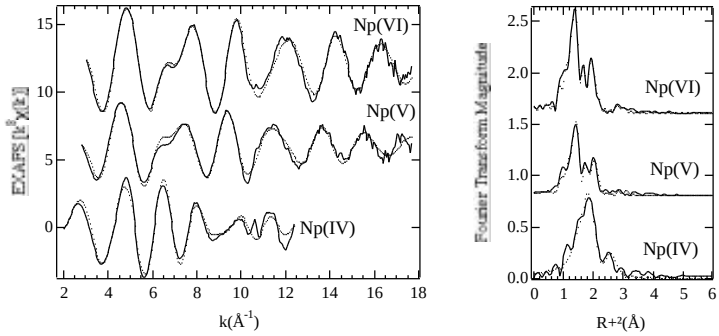

Fig. 3: Raw Np L(III)-edge k^3-weighted EXAFS spectra (left) and corresponding Fourier transforms (right) of 50 mM Np solutions. Solid line – experiment; dots – theoretical fit.

Both Np(V) and Np(VI) solutions Np2 and Np3 show the typical structural parameters of an actinyl ion. In case of Np(V), the distance to the axial oxygen atoms, O_{ax}, is 1.82 Å. In the equatorial plane the Np is surrounded by 4 water molecules with a Np-O_{eq} distance of 2.49 Å. The increase of the Np oxidation state from Np(V) to Np(VI) leads to a shortening of the axial and equatorial oxygen bonds by 0.07 Å and an increase of the number of water molecules attached to the neptunyl from four to five. The bond distances Np-O_{ax} and Np-O_{eq} of the Np(VI) solution are 1.75 Å and 2.42 Å, respectively.

The observed structural parameters for the Np-O bond distances of Np(IV) and Np(V) are in good agreement with the values reported for 5 mM Np in chlorine solution [11]. The structural parameters for Np(IV) sulfate and Np(VI) hydrate given in Tab. 1 are reported for the first time.

Tab. 1: EXAFS structural parameters for 50 mM Np solutions.

Sample	Shell	R(Å)	N	σ^2 (10^{-2} Å^2)
Np1, Np(IV)	Np-O	2.39	11.3(4)	1.18
	Np-S	3.07	2.2(3)	0.70
Np2 Np(V)	Np-O_{ax}	1.82	1.9	0.23
	Np-O_{eq}	2.49	3.6(2)	0.61
Np3 Np(VI)	Np-O_{ax}	1.75	2.0	0.15
	Np-O_{eq}	2.42	4.6(2)	0.56

Tc Model Solutions

The raw Tc K-edge k^3-weighted EXAFS spectra of two model solutions containing 127 mM and 1.3 mM TcO_4^- are shown in Fig. 4. The spectrum of the 127 mM Tc solution was recorded in a single sweep up to k=21 Å^{-1}. During this sweep the counting time per data point was gradually increased from 2 to 20 sec. It follows from the best theoretical fit to the data (Fig. 4) that Tc is surrounded by 4 oxygen atoms (N=4.1±0.1) at a distance of 1.72±0.01 Å (σ^2=0.0013±0.0004 Å^2). The EXAFS spectrum of the 100 times more dilute $NaTcO_4$(aq) sample is also shown in Fig. 4 and represents an average of four sweeps measured in fluorescence mode. The intensity of the Tc Kα fluorescence line was 1.2x10^5 counts/sec. The total count rate processed by the fluorescence detector was 6.4x10^5 counts/sec. Under these conditions, it was possible to analyze the Tc K-edge k^3-weighted EXAFS spectrum of the 1.3 mM Tc solution up to k=15 Å^{-1}. The structural parameters obtained are the same as for the TcO_4^- ion in the concentrated solution, i.e., N=3.9±0.2, R=1.72±0.01 Å, and σ^2=0.0016±0.0003 Å^2. These structural parameters agree with a previous Tc K-edge EXAFS measurement of a 200 mM NH_4TcO_4(aq) solution [12].

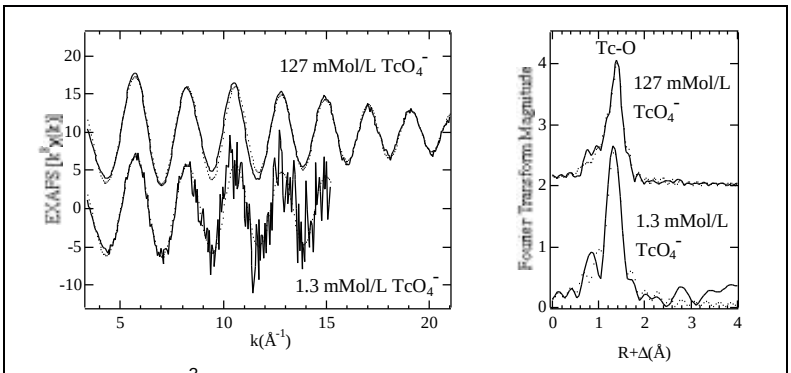

Fig. 4: Raw k^3-weighted Tc K-edge EXAFS spectra (left) and corresponding Fourier transforms (right) of experimental data (solid line) and theoretical fits (dots) for 127 mM (top) and 1.3 mM (bottom) $NaTcO_4$(aq).

These measurements on model solutions show the capability of ROBL to record EXAFS spectra over a large energy range covering at least two orders of magnitude in metal concentration due to the high degree of beam stability, which was achieved using an additional monochromator feed-back system. The possibility to record an EXAFS spectrum over 21 Å^{-1} as in the case of the 127 mM Tc solution, which is a record in itself, is of great practical importance. The ability to resolve neighboring atoms as individual coordination shells, i.e., the expected smallest interatomic distance known as resolution ΔR, is given by the ratio $\Delta R=\pi/2\delta k$, where δk is the k-range of the data. For the two spectra given in Fig. 4, the expected resolution ΔR is 0.09 and 0.13 Å, respectively.

U(VI) complexation with protocatechuic acid (PCA)

Figure 5 depicts the raw U L(III)-edge k^3-weighted EXAFS spectra and corresponding Fourier transforms of seven solutions with 1 mM U(VI) and 50 mM PCA as a function of pH ranging from 4.30 to 6.75. A significant change in the shape of the EXAFS with pH is observed in the k-range between 6 to 8 Å^{-1}. The structural parameters determined for the sample at pH 4.30 can be summarized as follows. The uranium is surrounded by two axial oxygen atoms, O_{ax}, at a distance of 1.79 ± 0.02 Å. The equatorial coordination shell consists of approximately 6 oxygen atoms, O_{eq}, with an U-O_{eq} distance of 2.45 ± 0.02 Å. This long U-O_{eq} distance is typical for bidentate coordination of the carboxylic group to the uranyl unit (see Fig. 6, left) [13, 14].

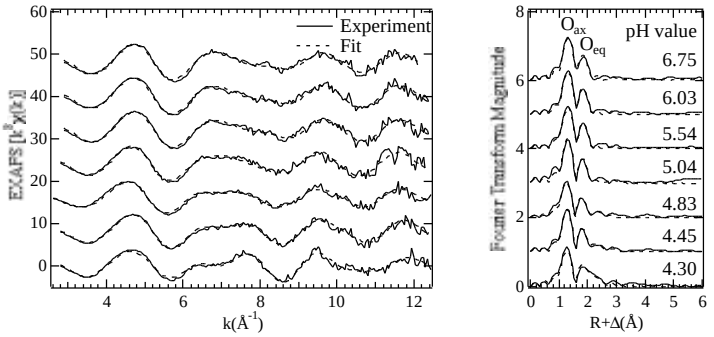

Fig. 5: Raw U L(III)-edge k^3-weighted EXAFS spectra (left) and corresponding Fourier transforms (right) of uranyl complexes with PCA as a function of pH.

As one can see from the Fourier transforms given in Fig. 5, the U-O_{eq} bond distance decreases with increasing pH. For the sample at pH 6.75, the U-O_{eq} bond distance is 2.36 ± 0.02 Å, i.e., almost 0.1 Å shorter than at pH 4.30. At high pH, the PCA ligands coordinate to the uranyl group in an o-diphenolic bonding fashion and the carboxylic group is not involved in the complex formation (see Fig. 6, right).

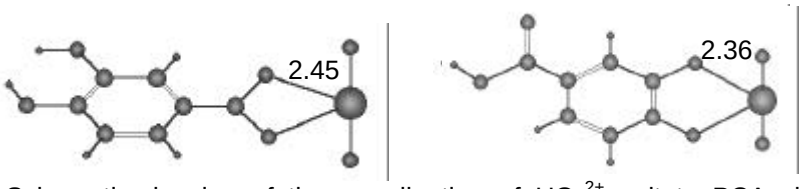

Fig. 6: Schematic drawing of the coordination of UO_2^{2+} unit to PCA via the carboxylic group (left) and the two phenolic hydroxyl groups (right). U - large spheres, C and O - medium spheres, H - small spheres. The numbers indicate the U-O_{eq} bond distances in Å.

Since the synchrotron beam probes the entire volume of the sample, the EXAFS spectrum is an average over all uranyl species present in the solution. If one assumes that the solutions at pH 4.30 and 6.75 contain only one uranyl species of different structures, it is possible to describe the EXAFS spectra at pH between 4.45 and 6.03 as a superposition of the EXAFS spectra of these two species. For pH 6.75 this assumption is supported by our previous EXAFS measurement of a sample at pH 10 where we observed similar structural parameters as at pH 6.76 [15]. The calculated contributions of the two coordination modes, i.e., bidentate-carboxylic and o-diphenolic, are shown in Fig. 7. At pH ~4.7 both uranyl complexes with PCA are equal in concentration. The bidentate coordination of the carboxylic COOH group dominates at pH lower than 4.7. However, above pH 4.7 the uranyl cation is predominantly coordinated by two neighboring phenolic OH groups as illustrated in Fig. 6.

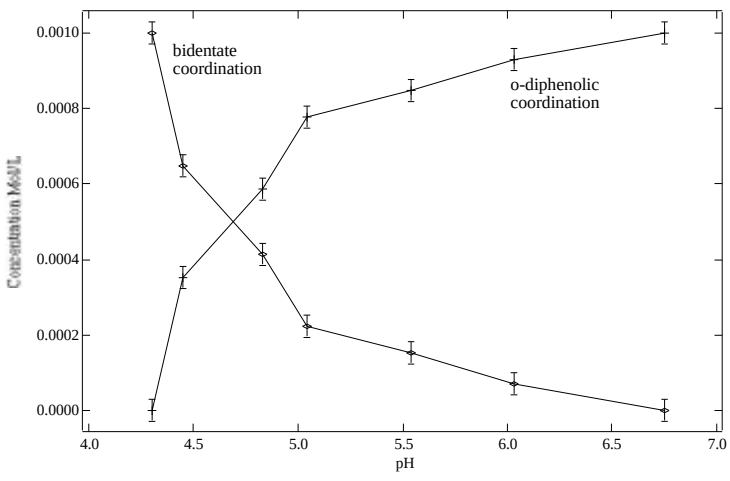

Fig. 7: Distribution of uranyl complexes derived from the EXAFS spectra given in Fig. 5.

The calculated species distribution given in Fig. 1 shows also a change around pH 4.7. The concentration of the 1:1 complex $[UO_2H_2L]^+$ decreases and that of the 1:2 complex $[UO_2HL_2]^{3-}$ increases. The agreement between the calculated (Fig. 1) and measured (Fig. 7) species distributions supports the complexation models used to extract the complexation constants from the potentiometric pH titration data.

This EXAFS study of uranyl complexation demonstrates the important role EXAFS spectroscopy can play for the validation of structural models, which are needed as input parameters for the determination of complexation constants from titration experiments. The molecular-level information obtained by EXAFS is essential for the validation of models that give a macroscopic description of the complexation. EXAFS analysis can also be used to validate or to suggest surface-complexation models that describe the interaction of radionuclides at mineral-water interfaces.

Summary and Conclusions

The following conclusions can be drawn from the EXAFS and XANES studies performed on Np, Tc, and U solutions at ROBL: 1) All EXAFS spectra measured in transmission mode in the energy range of 17 - 21 keV, which have a high signal-to-noise ratio, demonstrate the excellent performance of all beamline components including the synchrotron source, the monochromator and mirrors, sample positioners, and detectors. Based on the author's experience from radionuclide experiments on second-generation synchrotron light sources, we conclude that the large k-range and data quality that can be achieved at ROBL are superior. 2) EXAFS spectroscopy is a powerful technique to obtain structural information on radionuclide species in solutions. The EXAFS study on U(VI) complexation with PCA demonstrated the interplay between EXAFS and other techniques, in this case potentiometric pH titration. The complexation constants obtained by titration are needed to calculate the species distribution in order to prepare meaningful samples for EXAFS measurements. The molecular level information, which is the result of the EXAFS analysis, can be used to validate or to modify the underlying complexation models. 3) The actinide L(III)-edge XANES spectra are sensitive to the electronic and molecular structure of the actinide complexes and can be used to determine the oxidation state of the element under study [16]. XANES spectroscopy is especially valuable in cases where other analytical techniques, like UV/Vis spectroscopy, are limited due to matrix effects. 4) One disadvantage of performing experiments at a synchrotron light source is that the samples are usually prepared at the home institute and shipped to the experimental station, which can introduce unwanted changes in the sample composition during transportation. This is especially the case for experiments with radionuclides. At ROBL it is possible to overcome this disadvantage by preparing/modifying the radioactive samples in the glove box. For example, it is difficult to stabilize the Np(III) hydrate in solution. But with an electrochemical cell positioned in the synchrotron beam, it will be possible in the future to prepare the Np(III) oxidation state and to measure the XANES and EXAFS spectra in situ. Additional experimental possibilities, which are not discussed here, are available at ROBL for time-dependent and spatially-resolved XAFS studies using the monochromator in quick-EXAFS mode and by focusing the synchrotron beam [2]. In conclusion, the radiochemistry station at ROBL provides many unique features, which will contribute significantly to a better understanding of processes that are currently of great interest in environmental radiochemistry.

References

[1] R.J. Silva, H. Nitsche, Radiochim. Acta, **70/71** (1995) 377.
[2] W. Matz, et al., J. Synchrotron Rad., **6** (1999) in press.
[3] D.C. Koningsberger, R. Prins, *X-Ray Absorption: Principles, Applications, Techniques of EXAFS, SEXAFS and XANES*. John Wiley & Sons, New York, 1988.
[4] G.N. George, I.J. Pickering, Stanford Synchrotron Radiation Laboratory, EXAFSPAK: A Suite of Computer Programs for Analysis of X-Ray Absorption Spectra (1995).
[5] S.I. Zabinsky, J.J. Rehr, A. Ankudinov, R.C. Albers, M.J. Eller, Phys. Rev. B, **52** (1995) 2995.

[6] B. Johannsen, R. Jankowsky, B. Noll, H. Spies, T. Reich, H. Nitsche, L.M. Dinkelborg, C.S. Hilger, W. Semmler, Appl. Radiat. Isot., **48** (1997) 1045.
[7] R. Jankowsky, S. Kirsch, T. Reich, H. Spies, J. Inorg. Biochem., 70 (1998) 99.
[8] J.J. Bucher, P.G. Allen, N.M. Edelstein, D.K. Shuh, N.W. Madden, C. Cork, P. Luke, D. Pehl, D. Malone, Rev. Sci. Instrum., **67** (1996) 1.
[9] L. Baraniak, M. Schmidt, G. Bernhard, H. Nitsche, FZR Institute of Radiochmistry Annual Report 1996, (1997) 28.
[10] A.F. Hollemann, *Lehrbuch der anorganischen Chemie*. de Gruyter, Berlin, 1995.
[11] P.G. Allen, J.J. Bucher, D.K. Shuh, N.M. Edelstein, T. Reich, Inorg. Chem., **36** (1997) 4676.
[12] P.G. Allen, G.S. Siemering, D.K. Shuh, J.J. Bucher, N.M. Edelstein, C.A. Langton, S.B. Clark, T. Reich, M.A. Denecke, Radiochim. Acta, **76** (1997) 77.
[13] M.A. Denecke, T. Reich, S. Pompe, M. Bubner, K.H. Heise, H. Nitsche, P.G. Allen, J.J. Bucher, N.M. Edelstein, D.K. Shuh, J. Phys. IV France, **7** (1997) C2-637.
[14] M.A. Denecke, T. Reich, M. Bubner, S. Pompe, K.H. Heise, H. Nitsche, P.G. Allen, J.J. Bucher, N.M. Edelstein, D.K. Shuh, J. Alloys Compounds, **271-273** (1998) 123.
[15] A. Roßberg, T. Reich, C. Hennig, M.A. Denecke, L. Baraniak, H. Nitsche, FZR Institute of Radiochmistry Annual Report 1997, FZR-218 (1998) 72.
[16] S.D. Conradson, A. Al Mahamid, D.L. Clark, N.J. Hess, E.A. Hudson, M.P. Neu, P.D. Palmer, W.H. Runde, C.D. Tait, Polyhedron, **17** (1998) 599.